# 3D Printing of Carbides using Renewable Resources

Gabriel Carrillo[1], Morgan Sullivan[1], Monsur Islam[2] and Rodrigo Martinez-Duarte[2]

[1]Department of Materials Science and Engineering, Clemson University, Clemson, SC 29643

[2]Department of Mechanical Engineering, Clemson University, Clemson, SC 29634

## Abstract

Here we present our initial results for fabrication of 3D cellular architectures of tungsten carbide by 3D printing. We 3D printed cellular architectures of a biopolymer gel composite that consisted of iota-carrageenan and chitin as carbon precursors and tungsten tri-oxide as the tungsten source. The 3D printed gel composite was dried to obtain a 3D structure of biopolymer xerogel. Heat treatment of the xerogel structures resulted in 3D cellular architectures of porous tungsten carbide (WC). Significant shrinkage occurred during the drying and heat treatment process. The X-ray diffraction pattern confirmed that WC was formed after heat treatment. Scanning electron microscopy showed that the WC formed here featured a porous network of particle agglomerates. Ongoing work includes compressive testing to determine the Young's modulus of samples. A design of experiments will be implemented to develop a relationship between mechanical behavior and the geometry of the cellular architecture. Additionally, shrinkage, material solvent, printing substrate and filament diameter require further study to control rheology and increase precision during fabrication.

## Introduction

Carbides are useful materials due to the unique properties they show, such as high melting point, high chemical stability, high mechanical strength, low thermal expansion and low friction [1]. More specifically, porous carbides have low density, high surface area and high specific strength [2]. Many factors play into the production of carbides and their broad use in the engineering industry. Their synthesis is an important factor, as well as the cost and quality of the material. The carbothermal-reduction reaction (CRR) is the preferred synthesis technique in industry as it allows for various materials to be used as precursors [3]. In CRR, a metal oxide nanoparticle is reduced to its metallic element through heat treatment in an inert atmosphere in the presence of carbon. Carbide is then formed from the excess carbon reacting with the metallic element [4]. The current state of the art for the fabrication of carbide parts includes incomplete sintering and templating methods. However, these methods suffer from low sustainability as they depend on non-renewable carbon precursors. Furthermore, the shape of these carbide parts strongly depends on the use of a mold, and making a 3D complex shapes is challenging. Here, we postulate the fabrication of 3D complex shapes of porous carbide material by 3D printing of a biopolymer composite followed by carbothermal reduction reaction.

Additive manufacturing (AM) is a technology in which three-dimensional objects are made directly from CAD models by layer-upon-layer addition of material. This offers the ability to

fabricate more complex geometries when compared to subtractive manufacturing methods. Porous honeycomb structures used for filters in automobile engines serve as examples that are manufactured using molds [5]. Previous work in biopolymer shaping using AM includes fabricating tissue to replace damaged human body parts [6]. Several biopolymers have been used, such as collagen [7], gelatin [8], and alginate [9].

Presented here is the use of additive manufacturing of a biopolymer metal-oxide composite that upon heat treatment gets converted into complex carbide shapes. The biopolymers chitin and iota-carrageenan (IC) are the carbon sources present in the gel composite, and the metal-oxide is tungsten trioxide ($WO_3$). The viscosity of the gel can be manipulated through the concentration of iota-carrageenan present. The Bingham plastic nature of the composite allows it to be extruded and printed into various shapes at room temperature. We detail the initial results for 3D printing of cellular structures of tungsten carbide. We study the effect of printing parameters on the IC-Chitin based gel composite and the use of heat treatment to derive tungsten carbide (WC) structures. The shrinkage at different stages of this process is analyzed. We further characterize the heat-treated sample for material composition and microstructure.

## Experimental Section

### Materials

The biopolymer gel composite used in this work consisted of three components: IC (Sigma Aldrich, USA catalog number: C1138), chitin (Sigma Aldrich, USA catalog number: C9213) and 23-65 nm diameter tungsten trioxide nanoparticles (US Research Nanomaterials, Inc catalog number: US3540). The IC and chitin were the biopolymers as well as the carbon source. IC was the main thickening agent in the composite while chitin was meant to fill the gel network created by the IC. Together, these biopolymers created a gel substance while dissolved in aqueous solution that could be molded into various shapes. Tungsten trioxide was used as the metal-oxide in this composite. A Taz Lulzbot 5 3D printer was used along with a Discov3ry paste extruder. Cura software was chosen to prepare the computer-aided design (CAD) to be printed and control the parameters of the printer.

### Fabrication Protocol

IC and chitin dried powders were mixed in a weight ratio of 1:4. $WO_3$ metal-oxide nanoparticles were weighed as well and added to the powder mixture to acquire $WO_3$:C at a ratio of 1:4. Each powder was weighed individually on a balance and then combined using a vortex mixture (Thermo Scientific, Maximix M16710-33Q) for up to 10 minutes. Ultra-pure water was heated to 70 °C and added to the powdered mixture. The material was then homogenized to ensure a completely uniform mixture. The gel composite was put into a 60 mL syringe and inserted into the Discov3ry Paste Extruder that was connected to the printer. Vinyl-Flex (NSF-61) PVC 18-14 (1/8” x 1/4") tubing was attached to the syringe on one end, and a desired nozzle of 1.5 mm diameter was attached to the other end of the tube. The nozzle was then inserted into the holder on the printer.

To produce lightweight samples while retaining structural integrity, honeycomb structures served as the basis for designs used during the fabrication process. Prior studies have shown that this geometry increases the out-of-plane compressive and shear stresses that a structure can withstand [10]. Additionally, fabricating honeycomb structures permits the production of samples that are meant to represent unit cell structures that recur throughout an entire network. The compressive strength of structures containing various repeat units can be calculated based on the mechanical behavior of a single cell structure, which will occur in future studies. For this investigation, 3D printing occurred in the direction perpendicular to the plane of the honeycomb geometry in order to avoid overhangs that would have distorted the final product.

Designs for hexagonal honeycombs were generated in Solidworks, a CAD software. The CAD file of the structure was imported into the 3D printing software Cura, and the parameters were set as desired. After printing a given design, the sample was left to dry at room temperature for a minimum of 48 hours. Once dried, the sample was heat treated in a nitrogen atmosphere for 3 hours at 1300 °C.

Characterization

Measurements were taken of each sample after fabrication, shrinkage and heat treatment using the Dino-Lite Digital Microscope (Product number: AM4815ZT). Each sample was measured in three different spots on the sample to obtain an average of the line width using the software DinoCapture 2.0. The same line was measured after all three stages so that the amount of shrinkage could be calculated. The heat treated sample was characterized by X-ray diffraction (XRD) spectroscopy (Rigaku Ultima IV, Japan) to confirm the material composition. The microstructure of the heat treated sample was characterized by field emission scanning electron microscopy (FESEM, SU6600, Hitachi, Japan).

## Results and Discussion

Fabrication

A representative fabricated sample for hexagonal honeycomb geometries is shown in Figure 1a. Besides the geometric parameters of the 3D structures, other parameters that strongly influenced fabrication included nozzle size, printing substrate, material solvent, and filament diameter. This study focused on the quantitative evaluation of line width throughout production and made qualitative considerations for the printing substrate after drying. The image in Figure 1a shows that a perpendicular contact angle was maintained with the polycarbonate printing substrate after fabrication. Further studies will test whether or not a solvent's contact angle with a given substrate is maintained when extruded in combination with other reagents of the gel composite. Understanding this relationship should help predict the contact angle of the composite with the substrate after fabrication based on the contact angle of the solvent with the substrate by itself.

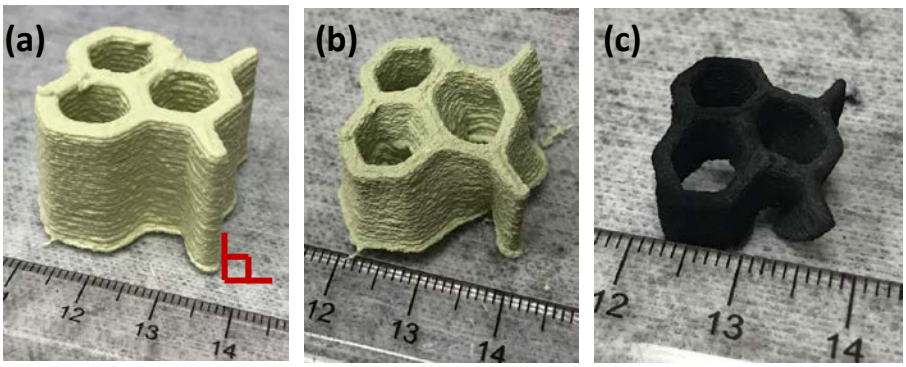


Figure 1: (a) 3D printed cellular architecture of a hexagonal honeycomb shaped biopolymer-$WO_3$ nanoparticle gel composite; (b) Hexagonal honeycomb shaped xerogel obtained after drying the 3D printed gel composite; (c) Hexagonal honeycomb shaped WC obtained after heat treatment of the xerogel at 1300 °C in nitrogen.

The data presented in Figure 2 summarizes the line width measurements that were obtained following the principal steps taken to obtain tungsten carbide with hexagonal honeycombs for this study. Figure 2 shows that the average measured width after fabrication for samples with designed line widths of 2 and 2.5 mm was roughly 0.5 mm greater than intended. In case of the sample with line width 3 mm, the designed line width was achieved. The increased precision for the 3 mm line width samples likely resulted from the fact that their dimensions were an even multiple of the 1.5 mm nozzle size. The 2 and 2.5 mm designed line widths were not even multiples of the nozzle width. This meant that the nozzle likely overcompensated when extruding material along its printing path since it needed to pass at least twice to achieve sample line widths greater than its own diameter.

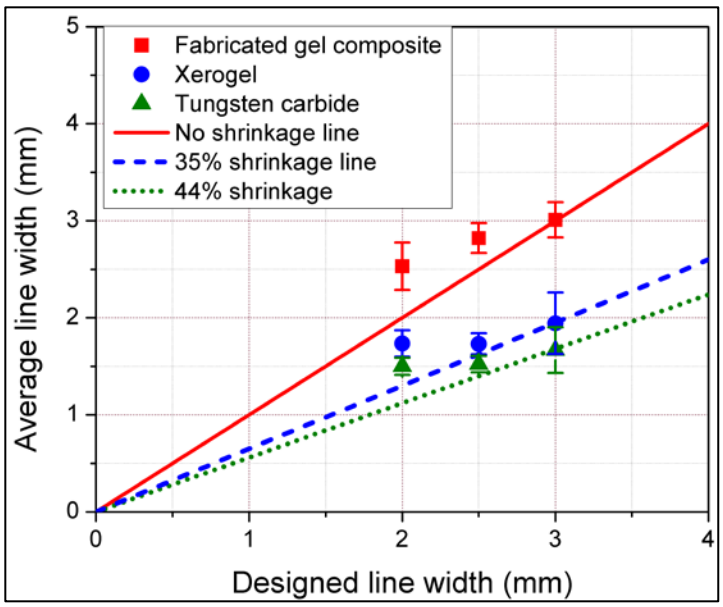


Figure 2: Summary relationship between average measured line width of a given sample and the corresponding designed width. Measurements were taken after fabrication, drying, and heat treatment. At least 3 samples were printed for each point. The error bars represent the standard deviation in the measurement.

Shrinkage

Upon drying, a xerogel structure of the honeycombs was obtained, as shown in Figure 1b. Following this step, all the samples exhibited an average shrinkage of 35.1 ± 3.6 % from the fabricated line width. The shrinkage was attributed to the evaporation of the water used to form the gel composite. The shape deformed during shrinkage and did not entirely form the desired shape once fully dried. This is indicated by the concavity of the sample's foundation in Figure 1b, which was not originally present after fabrication in Figure 1a. The concavity is further shown for samples with triangular honeycomb geometry in Figure 3.

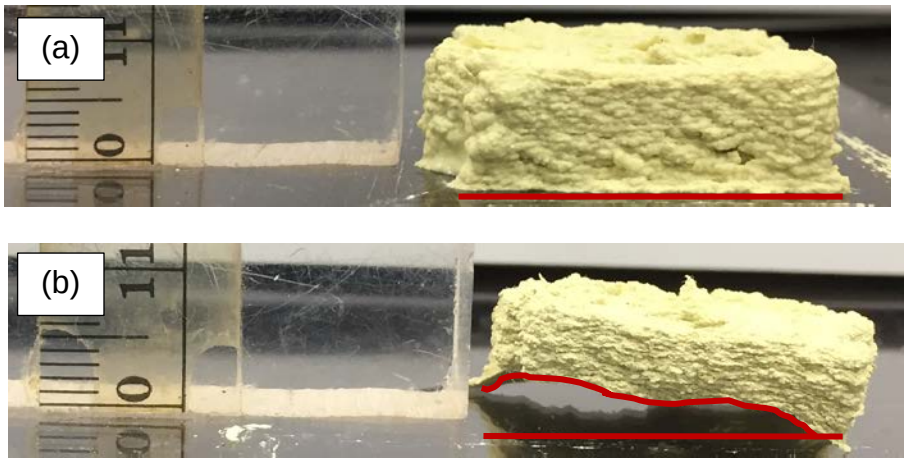


Figure 3: (a) 3D printed sample showing no deviation between the structure's foundation and the horizontal substrate; (b) Xerogel obtained after natural drying of the 3D printed gel composite showing the concave deformation that occurred during the drying process. This is indicated by deviation between the outline of the structure's foundation and the horizontal substrate.

The image in Figure 3a shows that the entire sample's foundation maintained contact with the polycarbonate printing substrate after fabrication. Figure 3b, however, shows concave deformation after drying that was also present for a sample of three-node geometry in Figure 1b. This deformation may have been due to the surface tension of the gel on the polycarbonate substrate. The contact angle after fabrication in Figure 3a appeared to be perpendicular, so the fact that the sample rises after drying suggests that the post-fabrication contact angle should have been obtuse in order for the sample to rise to a perpendicular orientation once the solvent had evaporated. Further study is needed to fully understand the causes of the deformation with respect to printing substrate and material solvent.

Heat Treatment

After heat treatment, the sample retained the same shape and deformation as it did before, but further shrinkage was observed. A representative heat treated sample is shown in Figure 1c. The average shrinkage of the heat treated samples was 43.8 ± 2.7% based on the designed width. The shrinkage during heat treatment was attributed to material loss during carbonization of the biopolymers, reduction of the $WO_3$ and carburization of the tungsten. It was confirmed that the material composition after heat treatment was tungsten carbide using X-ray diffraction characterization (XRD) shown in Figure 4a.

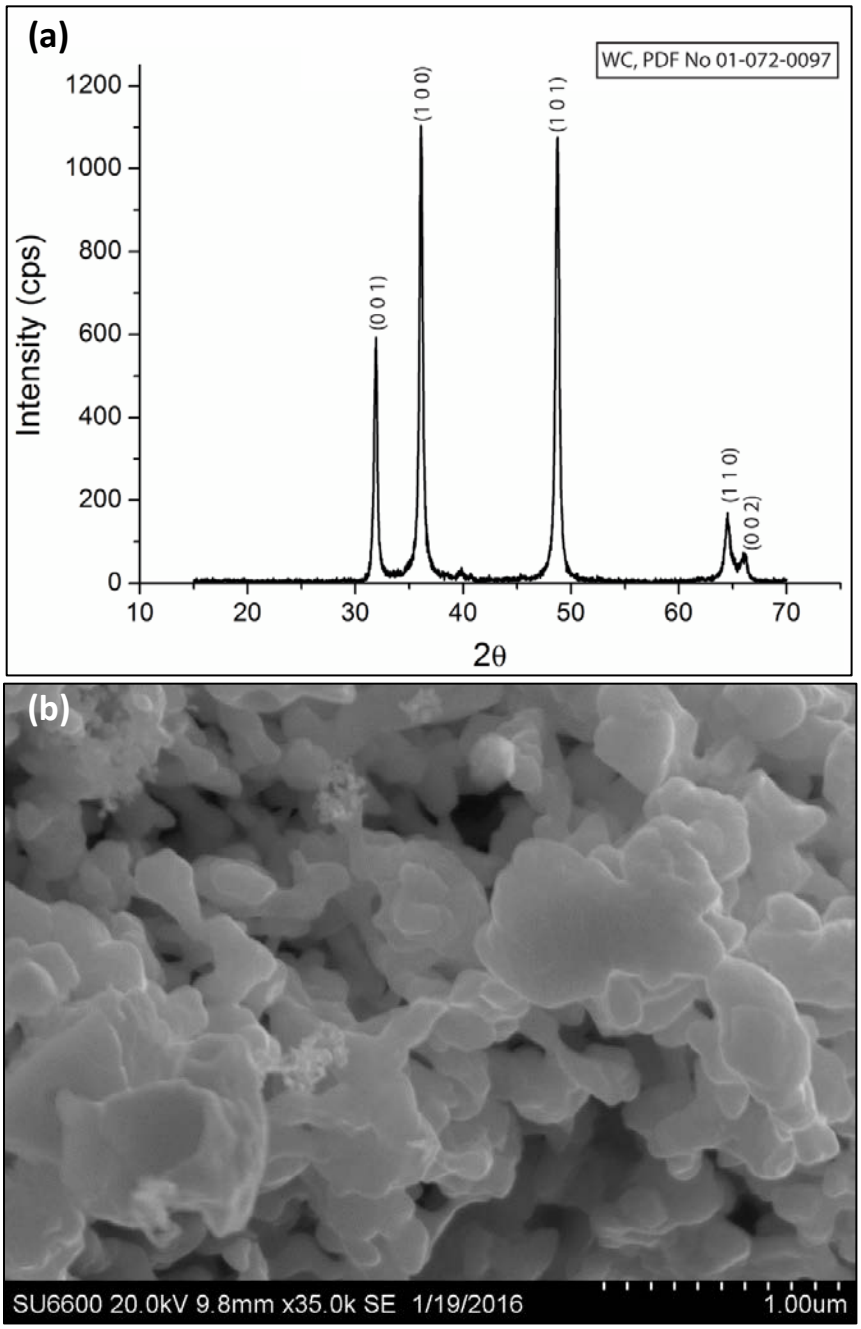


Figure 4: (a) The XRD pattern of the heat treated sample confirming the formation of WC; (b) SEM results showing microscopic agglomeration and porosity of the WC particles.

The major peaks were identified and labeled as the (001), (100), (101), (110) crystal planes of tungsten carbide. These signature peaks for WC are shown in Figure 1a. Peaks that corresponded to impurities were not observed. The results were in agreement with our previous report on the WC synthesis from this same IC-Chitin gel [1]. The FESEM image of the WC (Figure 4b) shows that a porous network of the agglomerated WC formed during heat treatment. The grain size of the WC was estimated as 20.15 ± 5 nm using the XRD and Scherrer equation (Equation 1). This equation was applicable to the material used in this study since the grain sizes

were smaller than 100 nm. The average grain size *D* was calculated using the X-ray wavelength $\lambda$, a constant *k*, the Bragg angle $\theta$ and the half width of the diffraction peak [11].

$$D = \frac{k\lambda}{Bcos\theta} \quad [1]$$

## Concluding Remarks

In this study, we presented the initial results for 3D printing of cellular material of tungsten carbide. We used a water-based gel composite consisting of iota-carrageenan and chitin biopolymers as the carbon source and $WO_3$ nanoparticle as the tungsten precursor. We successfully fabricated different honeycomb structures of the IC-chitin-WO3 gel composite. The fabrication process depended on each sample's line width as the primary parameter. 3D structures of the gel composite were dried to obtain 3D cellular structures of xerogel. Significant shrinkage occurred during the drying process due to the evaporation of water. Along with shrinkage, deformation occurred at the foundation of each sample due to perpendicular contact angles with the polycarbonate printing substrate during fabrication that ultimately deformed to a concave geometry after drying. Upon heat treatment, 3D cellular structures of tungsten carbide were obtained. The WC retained the shapes of the xerogel, although more significant shrinkage occurred due to the escape of volatile and gaseous substances during heat treatment.

Future work will include conducting mechanical testing on printed samples and identifying the impact that node, height, and line width of printed tungsten carbide have on the corresponding mechanical properties of a sample. In addition to this future work, the ratio of biopolymers and solvent will be altered to better understand each one's influence on polymer composite precursor rheology. This may include using different solvents with the biopolymer reagents. Making these modifications should assist in the goal of complex geometries that include overhangs in their design. Lastly, filament diameter and printing substrates will be studied in greater detail to see how these factors influence precision during fabrication and shrinkage after drying.

## Acknowledgements

Gabriel Carrillo, Morgan Sullivan and Rodrigo Martinez-Duarte acknowledge support from the Creative Inquiry program at Clemson University (Project 1138). Monsur Islam thanks the Hitachi High Technology Fellowship for enabling material characterization using electron microscopy.

## References

1. M. Islam, R. Martinez-Duarte, A sustainable approach for tungsten carbide synthesis using renewable biopolymers, Ceramics International 43 (2017) 10546-10553.
2. S. Shanmugam, D.S. Jacob, A. Gedanken, Solid state synthesis of tungsten carbide nanorods and nanoplatelets by a single-step pyrolysis, J. Phys. Chem. B. 109 (2005) 19056–19059.
3. J. Barker, M.Y. Saidi, J.L. Swoyer, A carbothermal reduction method for the preparation of electroactive materials for lithium ion applications, J. Electrochem. Soc. 150 (2003) A684. http://dx.doi.org/10.1149/1.1568936.
4. X. Guo, L. Zhu, W. Li, H. Yang, Preparation of SiC powders by carbothermal reduction with bamboo charcoal as renewable carbon source, J. Adv. Ceram. 2 (2013) 128–134.

http://dx.doi.org/10.1007/s40145-013-0050-4.
5. Ming C. LEU,Nannan GUO. Additive manufacturing: technology, applications and research needs[J]. Front Mech Eng, 2013, 8(3): 215-243.
6. Melchels, F. P. W., Domingos, M. a. N., Klein, T. J., Malda, J., Bartolo, P. J., and Hutmacher, D. W., 2012, "Additive manufacturing of tissues and organs," Prog. Polym. Sci., 37(8), pp. 1079–1104.
7. Stewart, R. L., Simpkins, M. W., Kachurin, A. M., Ph, D., Warren, W. L., and Williams, S. K., 2004, "Three- Dimensional BioAssembly Tool for Generating Viable Tissue-Engineered Constructs," Tissue Eng., 10(9), pp. 1566–1576.
8. Wang, X., Yan, Y., Pan, Y., Xiong, Z., Wu, R., Zhang, R., and Lu, Q., 2006, "Generation of Three- Dimensional Hepatocyte / Gelatin Structures with Rapid Prototyping System," Tissue Eng., 12(1), pp. 83-90.
9. S. Khalil, W. Sun, Bioprinting endothelial cells with alginate for 3D tissue constructs, J. Biomech. Eng. 131 (2009) 111002.
10. L. Wahl, S. Maas, D. Waldmann, A Zürbes, P. Frères, Shear stresses in honeycomb sandwich plates: Analytical solution, finite element method and experimental verification, Journal of Sandwich Structures & Materials 14 (2012) 449-468.
11. V. Richter, M. Ruthendorf, On hardness and toughness of ultra®ne and nanocrystalline hard materials, Int. J. Refract. Met. Hard Mater. 17 (2000) 141–152.